Nucleic Acids Research, 1996, Vol. 24, No. 12 **2377–2386**

Purification and characterization of the Pac1 ribonuclease of *Schizosaccharomyces pombe*

Giuseppe Rotondo and David Frendewey*

Department of Microbiology, New York University School of Medicine, 550 First Avenue, New York, NY 10016, USA

Received February 5, 1996; Revised and Accepted April 30, 1996

ABSTRACT

The *pac1*$^+$ gene of the fission yeast *Schizosaccharomyces pombe* is essential for viability and its overexpression induces sterility and suppresses mutations in the *pat1*$^+$ and *snm1*$^+$ genes. The *pac1*$^+$ gene encodes a protein that is structurally similar to RNase III from *Escherichia coli*, but its normal function is unknown. We report here the purification and characterization of the Pac1 protein after overexpression in *E.coli*. The purified protein is a highly active, double-strand-specific endoribonuclease that converts long double-stranded RNAs into short oligonucleotides and also cleaves a small hairpin RNA substrate. The Pac1 RNase is inhibited by a variety of double- and single-stranded polynucleotides, but polycytidylic acid greatly enhances activity and also promotes cleavage specificity. The Pac1 RNase produces 5′-phosphate termini and requires Mg^{2+}; Mn^{2+} supports activity but causes a loss of cleavage specificity. Optimal activity was obtained at pH 8.5, at low ionic strength, in the presence of a reducing agent. The enzyme is relatively insensitive to *N*-ethylmaleimide but is strongly inhibited by ethidium bromide and vanadyl ribonucleoside complexes. The properties of the Pac1 RNase support the hypothesis that it is a eukaryotic homolog of RNase III.

INTRODUCTION

Double-strand-specific ribonuclease activities (dsRNases) have been described from a variety of prokaryotic and eukaryotic sources, but few have been characterized in detail (1). The archetype of this class of enzymes is RNase III from *Escherichia coli* (2–4). RNase III is an endonuclease that usually makes staggered cuts in both strands of a double helical RNA, but in some cases it cleaves once in a single-stranded bulge in the helix (5,6). *In vitro*, the enzyme will degrade synthetic dsRNA to small oligonucleotides (7–9). Its primary biological function is the specific processing of rRNA and mRNA precursors (10,11); but it has also been implicated in other diverse phenomenon, such as mRNA turnover (4), conjugative DNA transfer (12), and antisense RNA-mediated regulation (13,14). The growing list of apparent homologs in the data bases (15,16) indicate that RNase III is highly conserved in both structure and function in bacteria. There have been many reports of dsRNase activities in eukaryotic cells, some of which exhibited properties consistent with a role in pre-rRNA processing (17,18), but the structure and biological significance of these enzymes is not known. The best candidates for eukaryotic RNase III homologs are the Rnt1 RNase from *Saccharomyces cerevisiae* (19), which is an essential pre-rRNA processing enzyme, and the Pac1 RNase from *Schizosaccharomyces pombe* (20,21).

The *S.pombe pac1*$^+$ gene was first identified by virtue of its ability to induce sterility in wild-type cells (20) or in a *pat1* mutant (21), which spontaneously initiates sexual development at the restrictive temperature (22,23). We isolated *pac1*$^+$ as a multi-copy suppressor of *snm1* (15), a mutant that maintains reduced steady-state levels of several small nuclear RNAs (snRNAs) (24). This genetic evidence suggests a role for *pac1*$^+$ in sexual development and snRNA metabolism, but its precise functions have not been determined. The *pac1*$^+$ gene encodes a protein of 363 amino acids whose carboxyl-terminal (C-terminal) two-thirds is very similar to *E.coli* RNase III (20,21). We showed that mutations that inactivate RNase III also abolish function when reproduced in the *pac1*$^+$ gene (15), which suggested a functional similarity between Pac1 and RNase III. Consistent with these genetic findings, expression of *pac1*$^+$ in *E.coli* produced an activity that converted dsRNA into acid soluble products (21); however, the double-strand specificity and other characteristics of this activity were not determined. To better understand the enzymatic behavior of the Pac1 RNase, we purified a poly-histidine-tagged version of Pac1 after overexpression in *E.coli*. We describe here the general biochemical properties of this enzyme, which is a highly active, double-strand-specific endoribonuclease.

MATERIALS AND METHODS

Plasmid construction

To create the tagged *pac1*$^+$ gene we amplified the Pac1 coding sequence by PCR with the following primers (NYU Pathology oligo service): 5′-cttggatccGGACGGTTTAAGAGGCAT-3′ (*Bam*HI site underlined; upper case are codons 2–7) and 5′-cgcaagcttTTAACGGGCAAACTTAGAG-3′ (*Hin*dIII site underlined; upper case are complementary to the the last base of codon 358, the last five codons, and the stop codon). The PCR product was cut with *Bam*HI and *Hin*dIII, cloned in pUC119, and its sequence confirmed by DNA sequencing. The same fragment

* To whom correspondence should be addressed

+Present address: Laboratoire du Metabolisme des ARN, Departement des Biotechnologies, Institut Pasteur, Paris, France

was transferred into pRSET-A (Invitrogen) to give pRSETpac. For expression in *S.pombe*, we first introduced an *Nde*I site at the initiating codon of the *pac1*$^+$ gene by site-directed mutagenesis as previously described (15). The modified *pac1*$^+$ gene was excised as a *Sac*I–*Hin*dIII fragment and inserted into pBluescript SK(–) (Stratagene) to create pBS-SKpac. The *Nde*I–*Hin*dIII fragment of pBS-SKpac was replaced with the *Nde*I–*Hin*dIII fragment of pRSETpac to create pBS-SKtPac. The tagged gene with its promoter was then moved as a *Sac*I–*Hin*dIII fragment into pIRT31 (15) to create pIRT31-tPac. To construct pREP1pac and pREP41pac, we excised the *Nde*I–*Hin*dIII fragment from pRSETpac, filled in its *Hin*dIII end, and inserted it into the *Nde*I and *Sma*I sites of pREP1 and pREP41 (25; gifts of D. Beach, Cold Spring Harbor Laboratory).

Purification of tPac1

We transformed BL21(DE3)pLysS [(F^- *ompT hsdS*$_B$($r_B^-m_B^-$) *gal dcm* (DE3) pLysS(Cm^R)] (Novagen) with pRSETpac and a single clone was grown at 30°C in 250 ml of tryptone-phosphate broth and induced with isopropylthio-β-D-galactoside (IPTG) exactly as described by Moore *et al.* (26). Three hours after induction, cells were collected by centrifugation and stored at –70°C. A native protein extract was prepared from the frozen cells and 10 ml was fractionated on a 1.8 ml Pro-Bond Ni-affinity column. Both extract preparation and chromatography were according to the instructions of the Xpress system kit (Invitrogen). The column was washed until the A_{280} was <0.01. Bound protein was eluted by consecutive application of 5 ml of elution buffer containing 50, 200, 350, and 500 mM imidazole. Fractions (1 ml) were collected and assayed for tagged Pac1 protein (tPac1) by Western blotting with an anti-T7•tag monoclonal antibody (mAb) (Novagen). tPac1 eluted in two peaks at 350 and 500 mM imidazole, which were pooled, concentrated with a Centricon-10 (Amicon) to a volume of 0.5 ml, diluted to 1.5 ml with storage buffer to a final composition of 500 mM NaCl, 20 mM sodium phosphate (pH 7.4), 67 mM imidazole, 1 mM dithiothreitol (DTT), 1 mM (ethylenedinitrilo)tetra-acetic acid (EDTA), and 30% glycerol, and stored at –20°C. The protein concentration measured with the Protein-Gold reagent (Integrated Separation Systems) and bovine serum albumin as the standard was 180 µg/ml. The purified enzyme has remained active for ~1 year but loses activity upon further dilution. A mock purification was performed on cells expressing the vector alone. The 350 and 500 mM imidazole fractions from the Ni-affinity column were monitored by Western blotting with an anti-RNase III serum (gift of B. Simons, UCLA) and were assayed for RNase III activity (27) with a ^{32}P-labeled dsRNA.

Immunological methods

To prepare anti-Pac1 serum, *E.coli* transformed with pRSETpac (see above) were grown at 37°C in 500 ml of LB broth (GIBCO BRL) containing 100 µg/ml ampicillin and 34 µg/ml chloramphenicol to an OD_{600} of 0.5, when tPac1 expression was induced with 0.6 mM IPTG. Three hours after induction, cells were collected by centrifugation, washed with 15 ml of 50 mM Tris–HCl (pH 8), 100 mM NaCl, 1 mM EDTA, and stored at –70°C. Frozen cells (3 g) were resuspended in 15 ml of lysis buffer (1% NP-40, 0.5% sodium deoxycholate, 0.1 M NaCl, 30 mM Tris–HCl, pH 8, 1 mM DTT, 1 mM EDTA); $MgCl_2$ (5 mM) and DNase I (10 µg/ml) were added, and the suspension was incubated on ice for 10 min. Inclusion bodies were collected by centrifugation at 10 000 *g* for 15 min, washed four times with lysis buffer and twice with 50 mM Tris–HCl (pH 8), 5 mM $MgCl_2$, 1 mM DTT, dissolved in 4.5 ml of loading buffer (28), and boiled for 10 min. One ml was fractionated by sodium dodecylsulfate polyacrylamide gel electrophoresis (SDS–PAGE) in a 12% gel. The tPac1 band, visualized by staining with 0.05% Coomassie brilliant blue R250 in water, was excised and sent to Cocalico Biologicals, Inc. (Reamstown, PA) for production of antibodies in rabbits.

For Western blot assays, proteins were separated by SDS–PAGE and transferred to nitrocellulose by semidry electroblotting (Owl Scientific). Blots were incubated with anti-T7•tag mouse mAb (1:10^4 dilution), anti-Pac1 rabbit serum (1:5 × 10^3), or anti-RNase III rabbit serum (1:10^4). Immune complexes were detected with alkaline-phosphatase-conjugated goat anti-mouse IgG (H+L; 1:10^4) or goat anti-rabbit IgG (Fc; 1:10^4) (Promega) and the CSPD chemiluminescence substrate according to the instructions of the Western-Light kit (Tropix). As controls, pre-immune rabbit serum replaced the anti-Pac1 and anti-RNase III sera or no first antibody was used.

Synthesis of double-stranded RNA substrates

The individual strands of the T3/T7 dsRNA (Fig. 1B) were transcribed from a template produced by PCR amplification of the fourth intron of the *S.pombe* β-tubulin gene (29; gift of M. Yanagida, Kyoto, Japan) with the following primers (synthesized by S. Teplin, Cold Spring Harbor Laboratory): 5′-gctcggaattaaccctcac-taaag*ggaacGTAGGTTTTTTTGCTTTC-3′, (T3 promoter in lower case, 5′ end of the intron in upper case) and 5′-ggtacctaatac-gactcactatag*ggagaCTACAGTCGTCAGTAC-3′ (T7 promoter in lower case, complement of the 3′ end of the intron in upper case). The transcription initiation sites are followed by asterisks. The PCR product was purified (30) and 40 ng was used in 20 µl transcription reactions containing 40 mM Tris–HCl (pH 7.9), 6 mM $MgCl_2$, 2 mM spermidine, 10 mM DTT, (50 mM NaCl for T3 reaction), 0.5 mM of each ribonucleoside triphosphate, 50 µCi [α-^{32}P]UTP (800 Ci/mmol; DuPont NEN), 20 U RNasin (Promega), and 20 U T3 or T7 RNA polymerase (Ambion) at 37°C for 1 h. The transcripts were prepared by DNase I (Promega) digestion, phenol extraction, and ethanol precipitation. The complementary RNAs were annealed and the unpaired ends removed by digestion with RNases A and T1 (Ambion) (31). The hybrid was gel-purified (32) and stored in diethyl pyrocarbonate(DEPC)-treated distilled water at –20°C. The RNase III substrate was a 63 bp dsRNA synthesized from pBluescript KS (Statagene). The N6 hairpin RNA (Fig. 1B) was transcribed according to Milligan *et al.* (33) in a 20 µl reaction containing 20 µCi [α-^{32}P]UTP (800 Ci/mmol), 1.25 pmol of synthetic DNA template (gift of A. Nicholson, Wayne State University, Detroit), and each ribonucleoside triphosphate at 1 mM and purified as described above. The purified N6 RNA was renatured by dissolving in 0.1 ml of 25 mM NaCl, 30 mM Tris–HCl (pH 7.6), heating at 90°C for 5 min, followed by slow cooling to room temperature and storage at –20°C. The radioactive RNAs were quantified by liquid scintillation counting in ScintiVerse BD (Fisher) and their concentrations calculated based on the specific activity of the labeling nucleotide and the expected number of radioactive phosphates in the RNA.

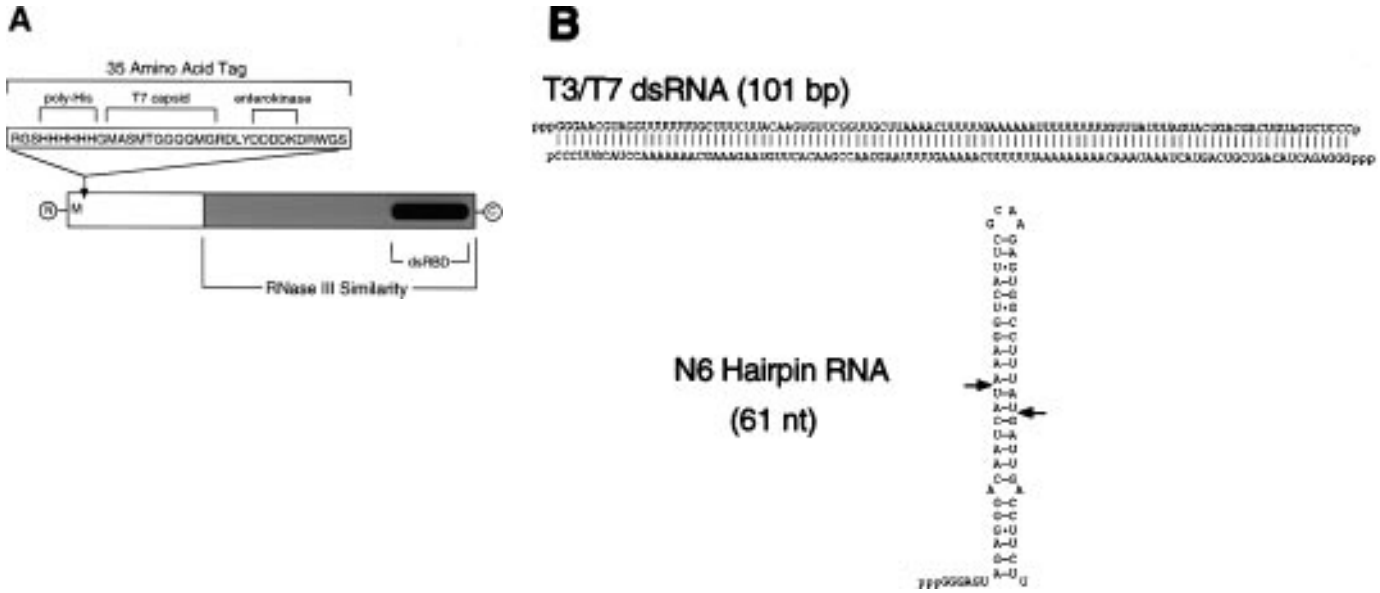

Figure 1. Structures of the tagged Pac1 protein and substrate RNAs. (**A**) The Pac1 protein is displayed as the large rectangle; *N* and *C* in circles refer to the N- and C-termini. The shaded area denotes the similarity with RNase III; the black oval represents the double-stranded RNA binding domain. The sequence of the 35 amino acid tag is shown above the Pac1 rectangle; its insertion site immediately adjacent to the initiating methionine (M) is indicated by the arrow. The amino acids constituting the His•tag, the T7•tag, and an enterokinase cleavage site are labeled with brackets. (**B**) The structure of the 101 bp T3/T7 dsRNA is that expected from its method of synthesis (Materials and Methods). The triphosphate 5′ ends are derived from the transcription initiating nucleotides; the 3′ monophosphate ends are produced by RNase cleavage. The expected secondary structure of the N6 hairpin RNA is shown. The *E.coli* RNase III cleavage sites (6) are indicated by arrows.

Pac1 RNase assays

Standard conditions were 30 mM Tris–HCl (pH 7.6), 5 mM $MgCl_2$, 1 mM DTT at 30°C. See figure legends for details of individual reactions. A theoretical relative molecular mass (M_r) of 45 504 was used to calculate tPac1 concentration. tPac1 was diluted in reaction buffer immediately prior to the start of the reaction. Reactions were assembled on ice and were started by the addition of 0.1 vol 50 mM $MgCl_2$. Polycytidylic acid [poly(C), Pharmacia] was added as indicated in the figure legends. Its concentration was calculated based on information supplied by the manufacturer on the average polymer length. For trichloroacetic acid (TCA) solubility assays, the reactions were stopped by addition of 0.5 ml of ice cold 5% TCA, and incubated on ice for 15 min. Aliquots (0.5 ml) were centrifuged at 16 000 *g* for 4 min in a Spin-X filter unit (Costar). Aliquots of the filtrate (0.4 ml) were quantified by liquid scintillation counting. For PAGE assays, reactions were stopped on ice by addition of an equal volume of 80% formamide, 0.1% xylene cyanol, 0.1% bromophenol blue, 12 mM EDTA. Aliquots (10 µl) were fractionated by electrophoresis on a polyacrylamide/7 M urea gel and the products detected by autoradiography. RNAs were excised and their radioactivity quantified by liquid scintillation counting.

To determine the optimal pH, product formation was assayed in Mes (2-[*N*-morpholino]ethanesulfonic acid), Bes (*N*,*N*-bis[2-hydroxyethyl]-2-aminomethanesulfonic acid), Hepes (*N*-[2-hydroxyethyl]piperazine-*N*′-[2-ethanesulfonic acid]), Tris (tris[hydroxymethyl]aminomethane), and Ches (2-[*N*-cyclohexyl]aminoethanesulfonic acid) at the following pH values: Mes, 5.5, 6.0, and 6.5; Bes, 6.5, 7.0, and 7.5; Hepes, 7.0, 7.5, and 8.0; Tris, 7.5, 8.0, and 8.5; Ches, 8.5, 9.0, and 9.5.

To analyze the 5′ ends of the Pac1 cleavage products, a 0.5 ml reaction containing 50 nM N6 RNA labeled with [α-^{32}P]GTP, 8 nM tPac1, 400 nM polycytidylic acid [poly(C)] (Pharmacia), 30 mM Tris–HCl (pH 7.5), 1 mM DTT, and 5 mM $MgCl_2$ was incubated for 30 min at 30°C. The RNA was collected by ethanol precipitation and fractionated by denaturing PAGE in a 12% gel. The three major products were excised, eluted, and co-precipitated with 10 µg of *E.coli* tRNA (Boehringer-Mannheim). One half of each product was digested with 5 U RNase T1, 0.25 µg of RNase A, and 0.5 U RNase T2 (Calbiochem) in 5 µl 10 mM Tris–HCl (pH 7.5), 1 mM EDTA at 37°C for 2 h. The digestion products were separated by thin layer chromatography (TLC) on polyethyleneimine(PEI)–cellulose (Fisher) in 1.75 M ammonium formate (pH 3.5) (34) along with unlabeled nucleotide mono-, di-, and tetraphosphate markers (Sigma). The markers were visualized by ultra-violet absorbance and the radioactive products by autoradiography with an intensifying screen. 5′-triphosphate-3′-monophosphate nucleotides were identified by PEI–cellulose TLC in 0.75 M potassium phosphate (pH 3.5) (35). For secondary analysis of the presumed [^{32}P]pGp digestion product, the spot was eluted from the TLC plate (36), mixed with 5 µg of *E.coli* tRNA, and digested with 5 µg nuclease P1 (Calbiochem) in 20 mM sodium acetate (pH 5.4) for 2 h at 37°C. P1 products were analyzed by PEI-cellulose TLC in 1 M LiCl (37).

Sequence alignment

The alignment of RNase III-like sequences shown in Figure 8 was assembled by manually adding new sequences to and extending our previously published alignment (15). New sequences were gleaned from the literature or found by a BLAST (38) search performed at the NCBI using the BLAST network service. The BLAST computation also revealed the repetition of blocks A and B in the unknown open reading frames from *S.pombe* and *Caenorhabditis elegans*.

RESULTS

Expression and purification of recombinant Pac1 RNase

To facilitate purification of the *S.pombe* Pac1 RNase, we inserted a tag between the first and second codons in the *pac1*$^+$ gene. The tag encodes 35 amino acids that include six contiguous histidines, as a nickel affinity ligand (His•tag), and part of the bacteriophage T7 gene 10 major capsid protein, as an epitope tag (T7•tag) (Fig. 1A). Expression of the tagged gene under the control of the normal *pac1*$^+$ promoter in *snm1* (24) and *pat1* (22,23) mutant *S.pombe* strains fully complemented their temperature sensitive growth defects. Thus, the tag does not impair Pac1 activity. To express the tagged protein (tPac1) in *E.coli* BL21(DE3)pLysS under the control of the inducible phage T7 promoter (39), we employed a method designed to produce soluble recombinant proteins (26). With this procedure ~50% of the tPac1 was soluble 3 h after induction with IPTG (Fig. 2A, lanes 3 and 4), while at later times after induction the protein became insoluble and extensive proteolytic breakdown occurred (not shown). Soluble tPac1 was purified from cell lysates by Ni-affinity chromatography (40). The purified protein migrates as a single prominent band with a M_r of ~50 000 by SDS–PAGE (Fig. 2A, lane 5). The apparent M_r, which is larger than the calculated molecular mass for tPac1 of 45.5 kDa, is consistent with the electrophoretic behavior of an untagged Pac1 protein expressed in *E.coli* (21) and identical to that obtained for tPac1 expressed in *S.pombe* (not shown). Purified tPac1 reacted with an anti-Pac1 serum (Materials and Methods) and with a mAb against the T7•tag (Fig. 2B). The tPac1 preparation contains several smaller polypeptides as minor components (Fig. 2A, lane 5). All of these were recognized by the anti-Pac1 serum (Fig. 2B, lane 2), while only the largest reacted with the anti-T7•tag mAb (Fig. 2B, lane 1), which suggests the smaller polypeptides are proteolytic breakdown products that have lost the epitope tag. If Pac1, like RNase III (27), is a dimer in its native state, polypeptides that lack the N-terminal tag might have bound to the column by association with the full length protein.

To establish that our tPac1 preparation was not contaminated with *E.coli* RNase III, we performed a mock purification from cells expressing the vector alone. [We were not able to achieve overexpression of soluble tPac1 in BL21(DE3)pLysS carrying a deletion of the *rnc* gene (provided by A. Nicholson).] We found by dsRNase assays and Western blotting (Fig. 2C, lane 1) that some of the endogenous RNase III bound to the Ni-affinity column. Despite this suggestion of possible RNase III contamination, we detected no reaction with the anti-RNase III antibody (Fig. 2C, lane 2) on a Western blot of ~300 ng of pure tPac1 (equivalent to the amount reacting with the anti-Pac1 antibody in lane 2 of Fig. 2B). The large amount of tPac1 in the extract from the overexpressing cells might occupy all of the available sites on the Ni-affinity resin and exclude interactions with RNase III. Thus, the purified tPac1 is essentially free of contaminating RNase III. The biochemical properties of the tPac1 RNase described below support this conclusion.

Optimization of Pac1 assay conditions

We initially assayed tPac1 by a modification of the standard TCA solubility assay used for RNase III (41). The substrate for these experiments was an internally labeled 101 bp (A+U)-rich dsRNA (T3/T7 dsRNA, Fig. 1B). tPac1 was able to convert the T3/T7

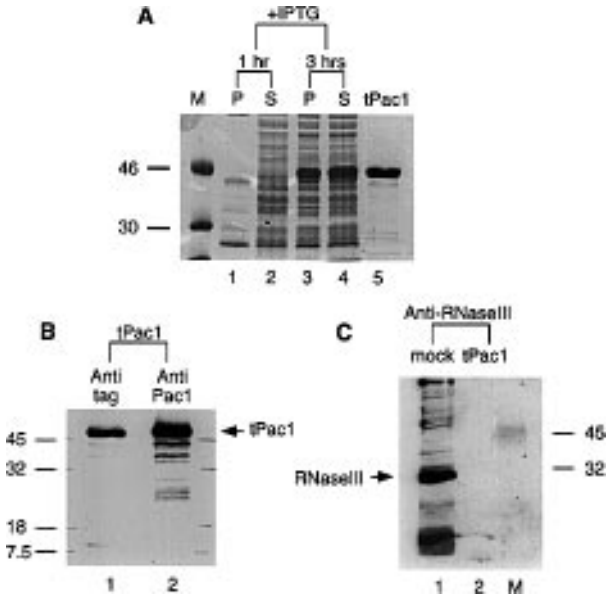

Figure 2. Purification of tPac1. (**A**) tPac1 expression in *E.coli* BL21(DE3)pLysS carrying pRSETpac and purification by Ni-affinity chromatography. Lanes 1–4, induction by IPTG. Aliquots of the culture (1 ml) were harvested at 1 or 3 h after IPTG addition as indicated above each lane. Insoluble (P) and soluble (S) proteins from whole cell lysates were fractionated by SDS–PAGE (12% polyacrylamide) and visualized by Coomassie blue staining. Lane 5, tPac1 purified by Ni-affinity chromatography. *M*, protein size markers; molecular masses in kilodaltons given at left. (**B**) Western blot analysis of purified tPac1. Lanes: 1, immunodetection by a mAb against the T7•tag; 2, immunodetection by anti-Pac1 serum. Mobilities and molecular masses of protein size markers given at left; position of tPac1 indicated by arrow at right. (**C**) Western blot analysis of purified tPac1 with anti-RNase III serum. Lanes: 1, protein eluted from the Ni-affinity column in the mock purification; 2, purified tPac1; M, protein size markers (molecular masses given at right); RNase III identified by arrow at left.

dsRNA to acid soluble products under the reaction conditions established for *E.coli* RNase III (27): 30 mM Tris–HCl (pH 7.6), 250 mM potassium glutamate, 10 mM $MgCl_2$, 5 mM spermidine, 1 mM DTT, 0.1 mM EDTA, and 0.4 mg/ml *E.coli* tRNA. These conditions were, however, very inefficient—only 30% of the input RNA was rendered acid soluble even when tPac1 was ~80-fold in excess of the substrate. To determine whether this activity was double-strand specific, we compared the degradation of the T3 strand, as a single-stranded substrate (ssRNA), against the T3/T7 dsRNA over a range of monovalent cation concentrations. This experiment (data not shown) demonstrated that at the lowest salt concentration the tPac1 RNase has a 10-fold preference for the T3/T7 dsRNA over the ssRNA substrate. Cleavage of the dsRNA was inhibited with increasing salt concentration. This inhibition was the same with the chloride and glutamate salts of potassium, which suggested that the cation was the inhibitory component. A divalent cation was essential, as no cleavage of either ds- or ssRNA was observed in the absence of $MgCl_2$. These experiments indicated that the RNase III conditions were not ideal for the tPac1 RNase. We therefore systematically altered the reaction components and temperature to achieve the highest dsRNase activity. This preliminary analysis yielded the following optimal reaction conditions: 30 mM Tris–HCl (pH 7.6), 1 mM DTT, 5 mM $MgCl_2$ at 30°C. Under these conditions dsRNase activity could be detected at tPac1

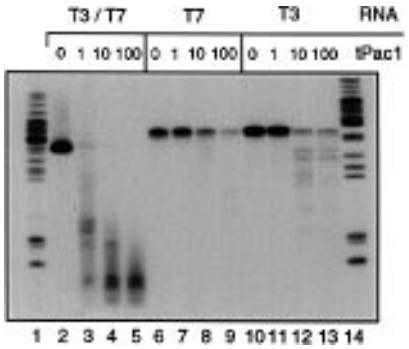

Figure 3. Cleavage of dsRNA versus ssRNA by the tPac1 RNase. ^{32}P-labeled T3/T7 dsRNA (lanes 2–5) and the T7 (lanes 6–9) and T3 (lanes 10–13) ssRNAs (~6 nM) were incubated for 10 min at 30°C in 20 µl reactions containing 30 mM Tris–HCl (pH 7.5), 25 mM KCl, 5 mM $MgCl_2$, 1 mM DTT, and tPac1 at the relative concentrations indicated above each lane (1 = 2 nM). One quarter of each reaction was analyzed by electrophoresis on a 10% polyacrylamide/7 M urea gel followed by autoradiography. Lanes 1 and 14 contain ^{32}P-labeled fragments from an *Msp*I digestion of pBR322. The DNA in lane 1 and the RNAs in lanes 2–5 were loaded native. The RNAs in lanes 6–13 and the DNA in lane 14 were heat-denatured before loading.

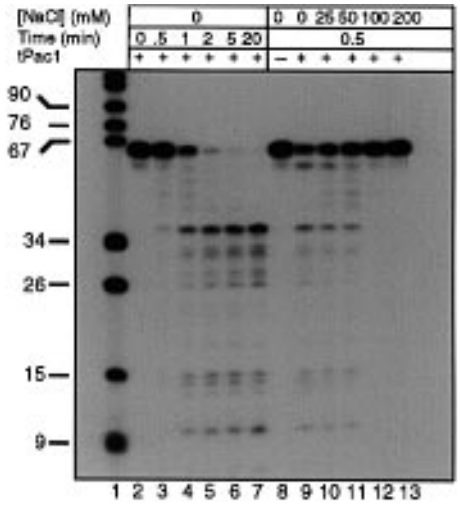

Figure 4. Cleavage of the N6 hairpin RNA by the tPac1 RNase. Lanes 2–7, a time course of N6 RNA cleavage. A 70 µl reaction with 21 nM [α-^{32}P]UTP-labeled N6 RNA (45 000 c.p.m.) and 4 nM tPac1 was incubated under standard conditions. At the times indicated above each lane, a 10 µl aliquot was removed and stopped. One half of each sample was analyzed by electrophoresis on a 12% polyacrylamide/7 M urea gel followed by autoradiography. Lanes 8–13, the effect of NaCl on N6 RNA cleavage. Reactions (10 µl) containing 22 nM [α-^{32}P]UTP-labeled N6 RNA (7000 c.p.m.) and 8 nM tPac1 were incubated for 0.5 min under standard conditions except that NaCl was added to the final concentrations indicated above each lane. The reactions were stopped and one half of each was analyzed on the same gel used for the time course. The reaction in lane 8 was a minus-enzyme control. DNA markers in lane 1 were as in Figure 3. All samples were heat-denatured before loading.

concentrations as low as 1 nM, and complete cleavage of a 20-fold molar excess of substrate was achieved in 10 min. We detected no dsRNase activity under RNase III conditions at tPac1 concentrations <40 nM. This result is consistent with the conclusion that *E.coli* RNase III is not a significant contaminant in our tPac1 preparation.

Cleavage properties of the Pac1 RNase

We used a gel assay to visualize the cleavage pattern produced by the tPac1 RNase. Cleavage of the T3/T7 dsRNA at three different tPac1 concentrations is shown in Figure 3 (lanes 2–5). At the lowest enzyme concentration (2 nM) nearly all of the T3/T7 dsRNA was converted to oligonucleotide products ranging in size from ~10 to 40 nt (lane 3). At higher enzyme concentrations the larger oligonucleotides were converted to 10–20 nt products (lanes 4 and 5). In contrast, the T7 and T3 single-stranded RNAs were poor substrates for the tPac1 RNase (lanes 6–13). A quantitative analysis of the cleavage efficiency revealed that 90% of the T3/T7 dsRNA was converted to oligonucleotide products at the lowest enzyme concentration, while cleavage of the T7 and T3 ssRNAs was detected only when tPac1 was 3–30-fold in excess of substrate (lanes 8, 9, 12 and 13). Different cleavage efficiencies were obtained with the two ssRNAs, which may reflect differences in secondary structure.

To examine the ability of the tPac1 RNase to cleave a single stranded RNA with a stable secondary structure, we tested the N6 hairpin RNA (Fig. 1B) as a substrate. The N6 RNA is an altered form (6) of the R1.1 *E.coli* RNase III processing signal found in the bacteriophage T7 early transcript (11). RNase III makes a staggered double strand break in the middle of the helix of N6 RNA (Fig. 1B) to produce three products: a 20 nt 5′ fragment, a 28 nt middle fragment composed of the upper half of the hairpin, and a 13 nt 3′ fragment (6). In contrast, the tPac1 RNase made multiple cleavages in the N6 RNA (Fig. 4, lanes 2–7); however, the initial products were not completely degraded. For example, a prominent product that migrated near the 34 nt DNA marker accumulated during the reaction and was not converted to smaller oligonucleotides at later times or with higher enzyme concentrations (not shown). This pattern implies that although the tPac1 RNase exhibits a relaxed cleavage specificity compared with RNase III (6), it appears to have preferred cleavage sites on N6 RNA (see below).

Effects of monovalent and divalent cations

To re-examine the inhibition of tPac1 RNase activity by monovalent cations, we assayed N6 RNA cleavage at several different NaCl concentrations. A 30 s reaction time was used to measure the initial reaction velocity. As seen with the T3/T7 dsRNA, N6 RNA cleavage was also inhibited by monovalent cations (Fig. 4, lanes 8–13). Substrate loss and product formation steadily decreased with increasing NaCl concentration. This experiment was repeated in triplicate and quantified by measuring formation of the major product (the fragment migrating slightly above the 34 nt DNA marker). Enzyme activity was barely detectable at 100 mM NaCl, while inhibition was complete at 200 mM. The NaCl concentration at half maximal inhibition was 75 mM. We observed nearly identical inhibitory effects with KCl and NH_4Cl (not shown).

To test whether other divalent metal ions can substitute for the Mg^{2+} requirement observed in our initial experiments, we assayed N6 RNA cleavage in reactions in which Mg^{2+} was replaced by Ca^{2+}, Zn^{2+}, Co^{2+}, Mn^{2+}, and Ni^{2+}. For this experiment we added poly(C), which enhances the activity and cleavage specificity of the tPac1 RNase with the N6 RNA substrate (see below). No cleavage of N6 RNA was observed without a divalent cation (Fig. 5, lanes 4 and 5). In the presence

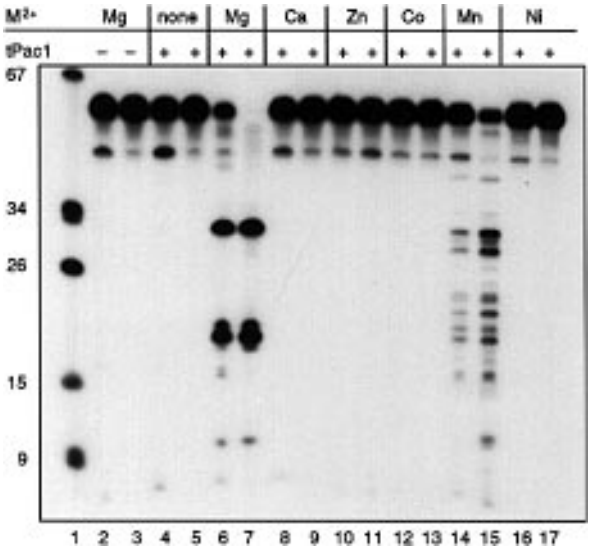

Figure 5. Effect of divalent cations on tPac1 RNase activity. Reactions (10 µl) containing 30 mM Tris–HCl (pH 7.6), 1 mM DTT, 400 nM poly(C), 50 nM [α-^{32}P]GTP-labeled N6 RNA (12 000 c.p.m.), and 8 nM tPac1 were incubated at 30°C for 20 s (lanes 2, 4, 6, 8, 10, 12, 14 and 16) or 10 min (lanes 3, 5, 7, 9, 11, 13, 15 and 17) without (lanes 4 and 5) or with the divalent cation (as the chloride salt at 5 mM) indicated above each lane. One half of each reaction was analyzed by electrophoresis and autoradiography as in Figure 4. Lanes 2 and 3, minus-enzyme controls; lane 1, DNA markers as in Figure 3.

of $MgCl_2$ three major products are formed (lanes 6 and 7). [Compare this pattern with the multiple cleavages in the absence of poly(C) shown in Figure 4.] Only Mn^{2+} could substitute for Mg^{2+}, but tPac1 RNase activity was reduced, compared with the Mg^{2+} reaction, and the specificity promoted by poly(C) was lost. The requirement for a divalent cation was not relieved by the polycation spermidine (not shown).

Effect of pH and small molecule inhibitors

To examine the pH optimum for tPac1 activity, we assayed the initial rate of N6 RNA cleavage at pH values between 5.5 and 9.5 in reactions buffered by Tris and the zwitter ionic buffers Mes, Bes, Hepes, and Ches. Three pH values—below, above, and near the pK_a—were assayed for each buffer. The tPac1 RNase exhibited a broad optimum between pH 8 and 9. We obtained the highest enzyme activity at pH 8.5 in Ches buffer; no activity was observed above pH 9.5 or below pH 6.5 (data not shown). Some differences among the buffers were observed. For example, the enzyme activity was slightly lower in Tris compared with the same pH in Ches or Hepes, and Bes was inhibitory.

The Pac1 coding sequence predicts a single cysteine residue located at a position that is part of the hydrophobic core of the double-stranded RNA binding domain (dsRBD) (16). To test if the sulfhydryl group in the unique cysteine is required, we assayed the effect of *N*-ethylmaleimide (NEM) on tPac1 RNase activity. This experiment confirmed that DTT is required for optimal tPac1 RNase activity and also showed that NEM was only mildly inhibitory (~60% inhibition at 10 mM). We found that 100 µM ethidium bromide caused complete inhibition of the tPac1 RNase, consistent with the enzyme's preference for dsRNA. No inhibition was observed at or below 0.1 µM, and half maximal inhibition was at ~3 µM. Vanadyl ribonucleoside complexes (VRC) are potent inhibitors of ribonucleases that are presumed to mimic the scissile phosphodiester bond in its trigonal bipyramid transition state (42). We found that VRC caused complete inhibition of tPac1 at 10 µM and exhibited half maximal inhibition at ~2 µM.

Effects of polynucleotides

The strong preference of the tPac1 RNase for dsRNA over ssRNA substrates prompted us to investigate the inhibitory properties of synthetic double- and single-stranded polynucleotides. Our initial experiments showed that the double stranded homopolymer poly(I)•poly(C) was a potent inhibitor of the T3/T7 dsRNA cleavage by tPac1. Consistent with the enzyme's dsRNA specificity, we found that poly(C) was not inhibitory, even at concentrations that were 100-fold in excess of substrate. In marked contrast, however, poly(I) inhibited tPac1 RNase activity as well as poly(I)•poly(C). To try to resolve these conflicting results, we examined the effect of a variety of polynucleotides on the rate of cleavage of N6 RNA. The results of this experiment confirmed the inhibition by poly(I)•poly(C) and poly(I) from another manufacturer and showed that homoribopolynucleotides of A, G and U, as well as the heteroduplex poly(rA)•poly(dT), inhibited tPac1 RNase activity. Three polynucleotides—poly(C), the mixed polynucleotide poly(U-C), and the DNA poly(dI)•poly(dC)—did not inhibit but actually simulated tPac1 RNase activity.

To examine the stimulatory effect of poly(C) in greater detail, we assayed tPac1 RNase activity with the N6 RNA substrate in the presence of increasing amounts of poly(C). The results of this experiment (Fig. 6A) demonstrate the dramatic enhancement of activity promoted by poly(C). Not only was there a quantitative effect but there was also a qualitative change in the cleavage pattern. In the absence of poly(C) the tPac1 RNase makes multiple cleavages in the N6 RNA (Fig. 6A, lane 3; see also Fig. 4). However, when poly(C) is present at 4 nM or above (Fig. 6A, lanes 4, 5, and 6, and Fig. 5, lanes 6 and 7), the cleavage pattern becomes more specific. Three predominant products are formed, indicative of two relatively precise cleavages in the helical stem. (The differences in the product band intensities in Figures 5 and 6A reflect the radioactive nucleotides in the substrates.) To measure the effect of poly(C) on enzyme activity we excised the upper hairpin product (see below for product assignments) from the gel shown in Figure 6A and quantified its radioactivity by liquid scintillation counting. The results plotted in Figure 6B (filled circles) demonstrate a steady increase in the rate of product formation with increasing poly(C) concentration. Since the amount of a particular product can reflect both enzyme activity and the choice of cleavage sites, we also assayed the percent of substrate cleaved (open circles) and found that poly(C) significantly enhances the cleavage rate even at low concentrations that do not promote increased cleavage specificity. Thus, poly(C) stimulates tPac1 RNase activity independently of its ability to promote more precise cleavage.

Cleavage chemistry

Cleavage of phosphodiester bonds by *E.coli* RNase III produces 5′ phosphoryl and 3′ hydroxyl ends on the products at the cleavage site (7–9). To determine whether the same was true for the tPac1 RNase, we purified the three major cleavage products

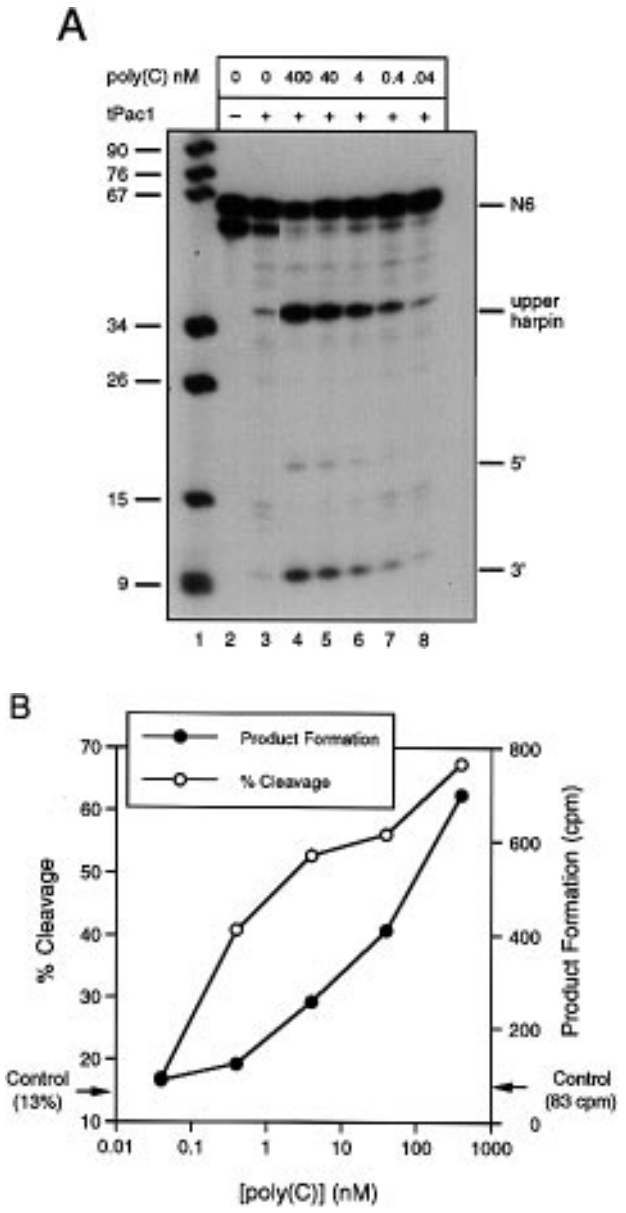

Figure 6. Stimulation of Pac1 RNAse by poly(C). [α-^{32}P]UTP-labeled N6 RNA (45 nM) was incubated with tPac1 (8 nM) for 30 s under standard conditions. Poly(C) was added at the concentrations indicated above each lane. (**A**) One half of each reaction was fractionated by electrophoresis in a 12% polyacrylamide/7 M urea gel and visualized by autoradiography. Lanes: 1, DNA markers as in Figure 3 (sizes in nt given at left); 2, a minus-enzyme control; 3, no poly(C); 4–8, poly(C) added at concentrations indicated above each lane. Substrate (N6) and products (upper hairpin, 5′, and 3′ fragments) are identified at right. (**B**) The substrate and upper hairpin product were excised from the gel and quantified by liquid scintillation counting. % cleavage is the proportion of substrate lost relative to the minus-enzyme control. Control values without poly(C) are indicated by arrows on the ordinate axes; the abscissa scale is logarithmic.

of [α-^{32}P]GTP-labeled N6 RNA (Fig. 5) and digested them with a combination of RNases A, T1 and T2, to reduce them to nucleoside-3′-monophosphates (Np). One of the N6 products should release the 5′ terminal tetraphosphate pppGp of the substrate RNA. The cleavage product that migrated between the 26 and 15 nt DNA markers (Fig. 5) released a labeled nucleotide upon RNase digestion that co-migrated by TLC with a product produced by digestion of the N6 substrate RNA (not shown). The migration of these digestion products relative to a ppppA marker indicated that they represented the 5′-terminal pppGp nucleotide of N6 RNA (36). Thus, the intermediate size product of N6 cleavage by the tPac1 RNase is the 5′ fragment. Labeling of this product was weaker with [α-^{32}P]UTP (Fig. 6A) than with [α-^{32}P]GTP (Fig. 5), while the reverse was true for the smallest N6 product. The largest product is equally intense with either label. From the sequence of N6 RNA, these data are consistent with the largest product being the upper hairpin fragment and the smallest being the 3′ fragment.

If the tPac1 RNase uses the same cleavage mechanism as RNase III, then the upper hairpin and 3′ fragment should release nucleoside-3′,5′-diphosphates (pNp) from their 5′ ends after RNase digestion. The major labeled product released from the 3′ fragment had a mobility by PEI–cellulose TLC that was very similar to the GDP marker (Fig. 7, lane 1), which tentatively identified it as pGp. The two minor spots could not be unambiguously identified from their mobilities, and their quantities were insufficient for further analysis. The upper hairpin product did not liberate a labeled pNp upon RNase digestion (not shown). The presumptive pGp spot produced from the 3′ fragment (Fig. 7, lane 1) was eluted and digested with nuclease P1 to remove the 3′ phosphate. The P1 digestion product co-migrated by PEI–cellulose TLC with GMP (Fig. 7, lane 2). These results established that the 3′ product of N6 RNA cleavage by tPac1 has a 5′ phosphoryl group attached to a guanosine at its 5′ end. Therefore, cleavage of phosphodiester bonds by the tPac1 RNase leaves a phosphate at the 5′ position. If tPac1 cleaved N6 RNA at the same site as RNase III, we would have expected a labeled Up mononucleotide as a digestion product of the 3′ fragment. We did not, however, detect a Up spot (Fig. 7, lane 1, and data not shown). These results and the electrophoretic mobility of the 3′ fragment relative to the DNA markers, are consistent with cleavage on the 5′ side of the last G in the N6 RNA. We have not mapped the second cleavage site, which we presume lies on the 5′ side of the stem in the secondary structure model of N6 RNA (Fig. 1B).

DISCUSSION

The enzymatic properties of the Pac1 RNase are very similar to RNase III. Both enzymes are double-strand-specific RNases that convert synthetic dsRNAs into short, acid soluble oligonucleotides (7–9) and leave 5′-phosphates on their cleavage products. The unit definition for RNase III is the amount of enzyme that will solubilize 1 nmol of acid precipitable polynucleotide phosphorus per hour (3). Using this definition, we estimate the specific activity of our tPac1 preparation to be 5×10^5 U/mg protein, which compares favorably with the 1.9×10^5 U/mg value for the most active RNase III preparation published (27). Since tPac1 appears to be fully functional in *S.pombe*, we are confident that the data we have obtained with the tagged protein accurately reflect the characteristics of the authentic Pac1 enzyme. The Pac1 RNase, like a dsRNase from calf thymus (18), differs from *E.coli* RNase III in its sensitivity to monovalent cations. In contrast, RNase III is actually stimulated by moderate concentrations of monovalent cations (2). At low monovalent cation concentrations, RNase III loses cleavage specificity

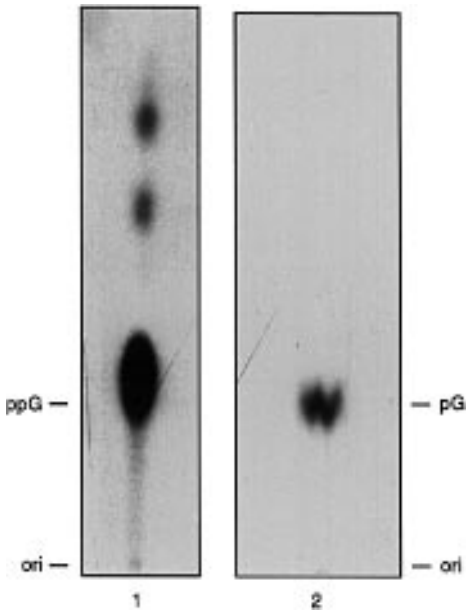

Figure 7. End group analysis of tPac1 cleavage products. A preparative reaction with [α-^{32}P]GTP-labeled N6 RNA was fractionated on a 12% gel. The smallest product (see Fig. 5) was purified and digested with RNases A, T1, and T2. (Panel **1**) An autoradiogram of the digestion products separated by TLC on PEI-cellulose in 1.75 M ammonium formate (pH 3.5). The presumed pGp spot was eluted and digested with nuclease P1. (Panel **2**) An autoradiogram of the P1 digestion products separated by TLC on PEI–cellulose in 1 M LiCl. The positions of the origins (ori) and the GDP (ppG) and GMP (pG) markers are indicated in the margins.

(3,6,27). We have not observed similar effects for Pac1. Like most of the dsRNases described (1), Pac1 has an absolute requirement for a divalent cation. Substitution of Mn^{2+} for Mg^{2+} causes Pac1 to lose cleavage specificity. A similar effect was reported for Mn^{2+} and Co^{2+} with *E.coli* RNase III (27). Despite the similarities in biochemical properties, Pac1 must possess important structural differences compared with its bacterial counterpart since our anti-Pac1 sera do not react with purified *E.coli* RNase III (G.R., unpublished observations) and anti-RNase III sera do not recognize tPac1 or the unmodified protein (21). With respect to functional equivalence, the *pac1*$^{+}$ gene can not suppress the *rnc105* mutation in the *E.coli* RNase III gene (*rnc*) (21) or a null allele (G.R., unpublished results). The *rnc* gene has not been tested for its ability to cure the *S.pombe snm1* and *pat1* mutants, which are complemented by *pac1*$^{+}$. However, overexpression of *rnc* in *S.cerevisiae* is lethal (43).

Under our standard conditions, the Pac1 RNase produces a cleavage pattern with the N6 hairpin RNA that suggests a mixture of random cuts and specific cleavages at preferred sites. However, when poly(C) is added 8–10-fold in excess of substrate, the cleavage pattern becomes much more specific. This enhanced specificity is accompanied by an ~8-fold increase in enzyme activity as assayed by the rate of specific product formation. The basis for these stimulatory effects is unclear. Two other polynucleotides—the mixed ribopolymer poly(U-C) and the DNA poly(dI)•poly(dC)—produced similar stimulatory effects, while all other polynucleotides tested were inhibitory. Perhaps Pac1 has an inherent affinity for cytidine-containing polynucleotides. The inhibition by polynucleotides was not consistent with Pac1's stringent preference for dsRNA substrates. For example, some single-stranded polymers, such as poly(I), were as potent inhibitors of the Pac1 RNase as poly(I)•poly(C).

The biochemical properties of the Pac1 RNase imply a functional homology with RNase III that is supported by the structural similarity. Pac1 is 25% identical over its C-terminal two-thirds to *E.coli* RNase III (20,21), and this relationship extends to other bacterial and eukaryotic RNase III-like proteins (15). Figure 8 shows an alignment of 13 protein sequences that share a marked similarity with RNase III. The sequences are arranged in three conserved blocks labeled A, B and C. In each block the first nine sequences are bacterial and the last four are eukaryotic. Blocks A and B surround the sites of the *rnc105* and *rnc70* mutations that inactivate both *E.coli* RNase III (4,44) and Pac1 (15). Block A is the N-terminal end of the RNase III similarity. The actual N-termini of the bacterial proteins lie ~20 amino acids upstream of the left end of block A. The N-termini of Pac1 and its *S.cerevisiae* homolog, Rnt1p (19), lie ~100 amino acids upstream. The last two sequences in Figure 8 (*Sp* orf and *Ce* orf) are part of very large open reading frames of unknown function in *S.pombe* and *C.elegans*. Their N-termini lie >1000 amino acids upstream. The C-termini of all the sequences lie not far beyond the right end of block C.

The glycine at the *rnc105* position in block A is conserved in all the sequences, and the adjacent amino acids form the most highly conserved stretch in the RNase III-like proteins. Block B surrounds the *rnc70* site, which is glutamic acid in all the sequences except that from *Bacillus subtilis* (*Bs rnc*), where it is replaced by lysine. A lysine at this position is surprising since the *rnc70* mutation converts the conserved glutamic acid to a lysine. Given that a transition at the first position is sufficient to convert a glutamic acid codon to one for lysine, a re-examination of the *B.subtilis* sequence may be warranted. Block C represents the putative dsRBD, which is required for the function of *E.coli* RNase III (44) and Pac1 (15). The bacterial dsRBD sequences, with the exception of that from *Mycoplasma genitalium* (*Mg rnc*), are clearly related and are good matches to the dsRBD consensus. Since the other *Mycoplasma* sequence shown [*M*(sp) orf] and another not shown (16) align well with the other bacterial sequences, the deviation in the *M.genitalium* sequence may be the result of a sequencing error that generated a frame shift. As noted previously (45), the Pac1 dsRBD is not a good match to the consensus except for the 20 amino acids at the C-terminus. This appears to hold true for the other eukaryotic sequences. The unknown *S.pombe* orf, however, deviates in an important way near its C-terminus. A pair of alanines in this region are found in nearly all dsRBDs (46), and changing these alanines to valines abolishes Pac1 function (15). This result is consistent with the structural models of the dsRBD, which predict that bulky side groups are not tolerated at these positions (16,47). Thus, the absence of this alanine pair in the *S.pombe* orf suggests either a sequencing error or a protein with poor dsRNA binding properties.

The two orfs of unknown function from *S.pombe* and *C.elegans* are more closely related to one another than they are to other RNase III sequences. These orfs predict proteins with interesting dual functions. The RNase III-like domain is contained within ~300 amino acids at the C-terminal end of each protein. Blocks A and B are separated by a variable number of amino acids not found in the other RNase III sequences. In addition, blocks A and B, but not C, are repeated immediately upstream of the complete RNase III-like domains. This reiteration is indicated by the upper of the two lines of sequence shown for the *S.pombe* and *C.elegans*

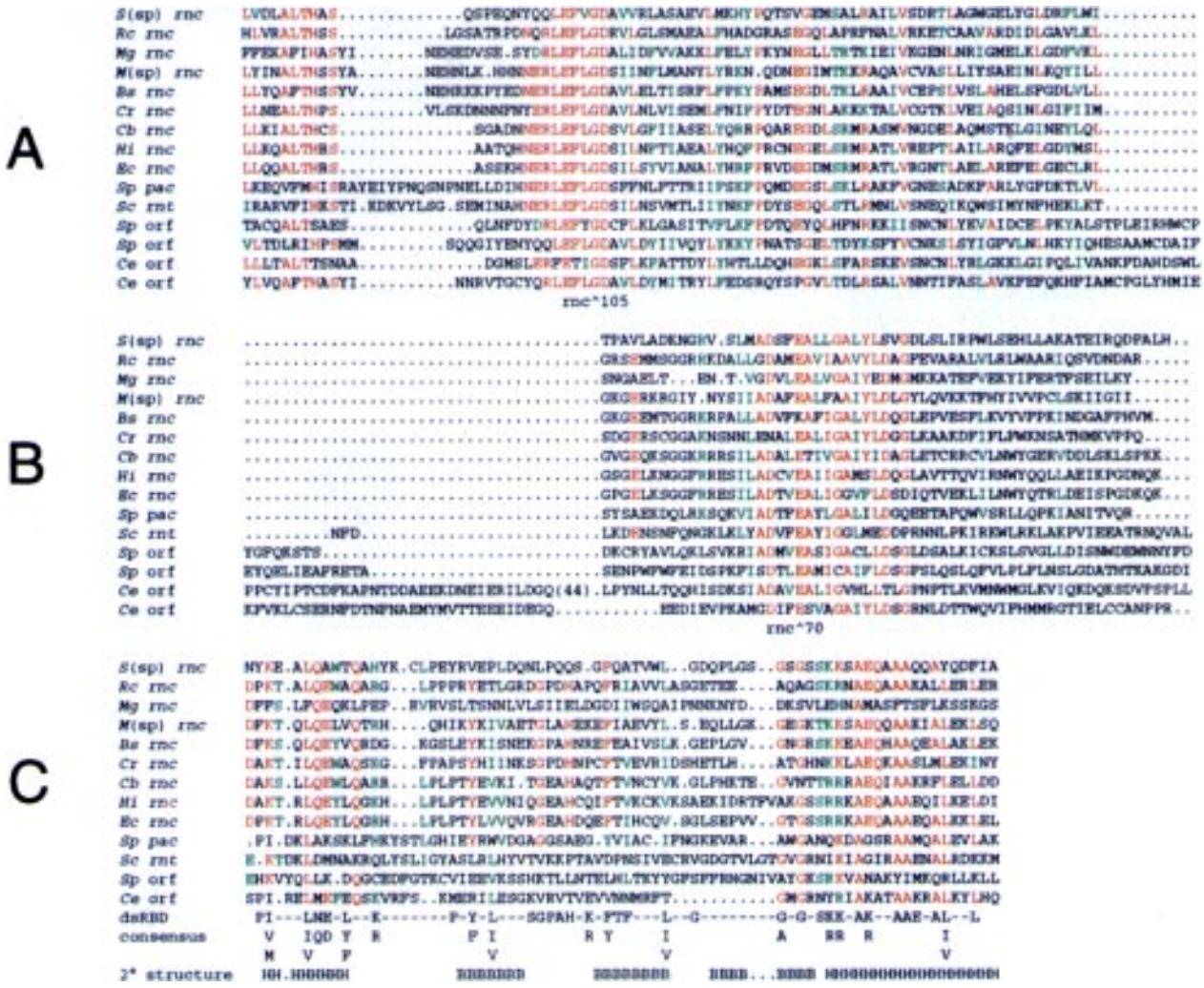

Figure 8. Alignment of RNase III-like sequences. The RNase III-like domains of nine bacterial (upper rows in each block) and four eukaryotic (lower rows) protein sequences are aligned in three blocks labeled A, B and C. Other than the division between prokaryotic and eukaryotic, the order of the sequences is arbitrary. Red letters indicate positions that are identical in a majority of the sequences; green letters denote amino acids that are chemically similar in a majority of the sequences according to the following groupings: (L, I, V); (F, Y, W); (N, Q); (K, R, H); (D, E); and (S, T). A dsRBD consensus and secondary structural features of the dsRBD of*E.coli* RNase III (16) are given below block C; H, α-helix; B, β-strand. The bacterial sequences are a representative sample, while the eukaryotic sequences are all that were found in a search for RNase III-like sequences. The sites of the *E.coli rnc105* and *rnc70* mutations are marked under blocks A and B. Sequences are identified with their accession numbers as follows: *S*(sp), gene slr0346 of a *Synechocystis* species of Cyanobacteria, D64000 (52); *Rc*, *Rhodobacter capsulatus*, Z68305 (53); *Mg*, *Mycoplasma genitalium*, U39721 (50); *M*(sp), unknown Mycoplasma-like species, U15224 (16); *Bs*, *Bacillus subtilis*, D64116 (54); *Cr*, *Cowdria ruminantium*, a Rickettsial species, X58242 (55); *Cb*, *Coxiella burnetii*, a Rickettsial species, L27436 (56); *Hi*, *Haemophilus influenzae*, P44441 (57); *Ec*, *E.coli*, X02946 (44); *Sp pac*; Pac1, X54998 (20,21); *Sc rnt*; *S.cerevisiae* Rnt1p, U27016 (19); *Sp* orf, orf SPAC8A4.08c on *S.pombe* chromosome I, Z66569 (58); *Ce* orf, orf CELK12H4.1 from *Caenorhabditis elegans*, L14331 (59). There are two lines for the *Sp* and *Ce* orfs in blocks A and B because of a repetition of these domains (see text). The lower of the two lines is continuous with block C.

orfs in blocks A and B in Figure 8. The large (900–1200 amino acids) N-terminal regions of the two orfs share a similarity (not shown) with the DEAD box family of RNA-dependent ATPases/helicases (48). The canonical DEAD motif is replaced by the sequence DECH in the *S.pombe* and *C.elegans* orfs. A similar duality of structure is seen in the human RNA helicase A and *Drosophila maleless* proteins, each of which has two N-terminal dsRBDs upstream of a central DEAH helicase domain (49). The unusual structure of the *S.pombe* and *C.elegans* orfs suggests enzymes that can both unwind and cleave dsRNA. Eukaryotic cells may, therefore, have more than one type of RNase-like dsRNase. *S.cerevisiae* Rnt1p is a pre-rRNA processing enzyme (19). The similarity between Rnt1p and Pac1 suggests that the *S.pombe* enzyme might also participate in rRNA maturation. Since a *pac1* null mutation is lethal (21), the second RNase III-like gene in *S.pombe* may not be able to substitute for Pac1's essential function in rRNA synthesis. Conversely, the observed effects of Pac1 overexpression on fertility (20,21) and snRNA metabolism (15) may reflect its ability to compensate for loss or normal attenuation of the function of the large *S.pombe* RNase III-like protein.

The retention of an RNase III gene in the minimal genome of *Mycoplasma genitalium* (50) and its conservation in bacteria and eukaryotes implies an ancient and important function. The

possibility of multiple forms of RNase III and the emerging involvement of dsRNA in cell growth, differentiation, and development (1,51) raise the possibility that RNase III-like enzymes play critical regulatory roles in eukaryotic cells.

ACKNOWLEDGEMENTS

We thank Allen Nicholson, Bob Simons, Ron Beavis, Mitsuhiro Yanagida and David Beach for generous gifts of materials and strains, Naoko Tanese for crucial advice on protein expression in *E.coli*, Warren Jelinek for assistance in the preparation of TEAB and, along with Jim Borowiec, for critical comments on the manuscript, and Pam Cowin for cogent editorial suggestions. We thank Manuel Ares for communication of results before publication. This work was supported by Bridging Funds from the New York University Medical Center and by Developmental Funds from the Center for AIDS Research at NYU. D.F. was supported by a Whitehead Fellowship for Junior Faculty and an Irma T. Hirschl Career Scientist Award.

REFERENCES

1 Nicholson, A. W. (1996) *Prog. Nucleic Acids Res. Mol. Biol.*, **52**, 1–65.
2 Robertson, H. D., Webster, R. E. and Zinder, N. D. (1968) *J. Biol. Chem.*, **243**, 82–91.
3 Dunn, J. J. (1982) In Boyer, P. D. (ed.), *The Enzymes.* Academic Press, New York, Vol. 15, Part B, pp. 485–499.
4 Court, D. (1993) In Brawerman, G., and Belasco, J. (eds.), *Control of mRNA Stability.* Academic Press, New York, pp. 70–116.
5 Robertson, H. D. (1982) *Cell*, **30**, 669–672.
6 Chelladurai, B., Li, H., Zhang, K. and Nicholson, A. W. (1993) *Biochemistry*, **32**, 7549–7558.
7 Schweitz, H. and Ebel, J. P. (1971) *Biochimie*, **53**, 585–593.
8 Crouch, R. J. (1974) *J. Biol. Chem.*, **249**, 1314–1316.
9 Robertson, H. D. and Dunn, J. J. (1975) *J. Biol. Chem.*, **250**, 3050–3056.
10 Young, R. A. and Steitz, J. A. (1978) *Proc. Natl. Acad. Sci. USA*, **75**, 3593–3597.
11 Dunn, J. J. and Studier, F. W. (1973) *Proc. Natl. Acad. Sci. USA*, **70**, 3296–3300.
12 Koraimann, G., Schroller, C., Graus, H., Angerer, D., Teferle, K. and Hogenauer, G. (1993) *Mol. Microbiol.*, **9**, 717–727.
13 Gerdes, K., Nielsen, A., Thorsted, P. and Wagner, E. G. (1992) *J. Mol. Biol.*, **226**, 637–649.
14 Blomberg, P., Wagner, E. G. H. and Nordström, K. (1990) *EMBO J.*, **9**, 2331–2340.
15 Rotondo, G., Gillespie, M. and Frendewey, D. (1995) *Mol. Gen. Genet.*, **247**, 698–708.
16 Kharrat, A., Macias, M. J., Gibson, T. J., Nilges, M. and Pastore, A. (1995) *EMBO J.*, **14**, 3572–3584.
17 Grummt, I., Hall, S. H. and Crouch, R. J. (1979) *Eur. J. Biochem.*, **94**, 437–443.
18 Ohtsuki, K., Groner, Y. and Hurwitz, J. (1977) *J. Biol. Chem.*, **252**, 483–491.
19 Abou Elela, S., Igel, H. and Ares, M., Jr. (1996) *Cell*, **85**, 115–124.
20 Xu, H.-P., Riggs, M., Rodgers, L. and Wigler, M. (1990) *Nucleic Acids Res.*, **18**, 5304.
21 Iino, Y., Sugimoto, A. and Yamamoto, M. (1991) *EMBO J.*, **10**, 221–226.
22 Iino, Y. and Yamamoto, M. (1985) *Mol. Gen. Genet.*, **198**, 416–421.
23 Nurse, P. (1985) *Mol. Gen. Genet.*, **198**, 497–502.
24 Potashkin, J. and Frendewey, D. (1990) *EMBO J.*, **9**, 525–534.
25 Basi, G., Schmid, E. and Maundrell, K. (1993) *Gene*, **123**, 131–136.
26 Moore, J. T., Uppal, A., Maley, F. and Maley, G. F. (1993) *Protein Express. Purific.*, **4**, 160–163.
27 Li, H.-L., Chelladurai, B. S., Zhang, K. and Nicholson, A. W. (1993) *Nucleic Acids Res.*, **21**, 1919–1925.
28 Laemmli, U. K. (1970) *Nature*, **227**, 680–685.
29 Hiraoka, Y., Toda, T. and Yanagida, M. (1984) *Cell*, **39**, 349–358.
30 Frendewey, D., Barta, I., Gillespie, M. and Potashkin, J. (1990) *Nucleic Acids Res.*, **18**, 2025–2032.
31 Manche, L., Green, S. R., Schmedt, C. and Mathews, M. B. (1992) *Mol. Cell. Biol.*, **12**, 5238–5248.
32 Saccomanno, L. and Bass, B. L. (1994) *Mol. Cell. Biol.*, **14**, 5425–5432.
33 Milligan, J. F. and Uhlenbeck, O. C. (1989) *Methods Enzymol.*, **180**, 51–62.
34 Randerath, K., Gupta, R. C. and Randerath, E. (1980) *Methods Enzymol.*, **65**, 638–680.
35 Goody, R. S. and Eckstein, F. (1971) *J. Am. Chem. Soc.*, **93**, 6252–6257.
36 Frendewey, D., Dingermann, T., Cooley, L. and Söll, D. (1985) *J. Biol. Chem.*, **260**, 449–454.
37 Greer, C. L. (1994) In Higgins, S. J., and Hames, B. D. (eds.), *RNA Processing, a Practical Approach.* IRL Press, Oxford, Vol. II, pp. 173–209.
38 Altschul, S. F., Gish, W., Miller, W., Myers, E. W. and Lipman, D. J. (1990) *J. Mol. Biol.*, **215**, 403–410.
39 Studier, F. W., Rosenberg, A. H., Dunn, J. J. and Dubendorff, J. W. (1990) *Methods Enzymol.*, **185**, 60–89.
40 Van Dyke, M. W., Sirito, M. and Sawadogo, M. (1992) *Gene*, **111**, 99–104.
41 Robertson, H. D. (1990) *Methods Enzymol.*, **181**, 189–202.
42 Lienhard, G. E., Secemski, I. I., Koehler, K. A. and Lindquist, R. N. (1972) *Cold Spring Harbor Symp. Quant. Biol.*, **36**, 45–51.
43 Pines, O., Yoon, H. J. and Inouye, M. (1988) *J. Bacteriol.*, **170**, 2989–2993.
44 Nashimoto, H. and Uchida, H. (1985) *Mol. Gen. Genet.*, **201**, 25–29.
45 St. Johnston, D., Brown, N. H., Gall, J. and Jantsch, M. (1992) *Proc. Natl. Acad. Sci. USA*, **89**, 10979–10983.
46 Burd, C. G. and Dreyfuss, G. (1994) *Science*, **265**, 615–621.
47 Bycroft, M., Grünert, S., Murzin, A. G., Proctor, M. and St. Johnston, D. (1995) *EMBO J.*, **14**, 3563–3571.
48 Linder, P., Lasko, P. F., Ashburner, M., Leroy, P., Nielsen, P. J., Nishi, K., Schnier, J. and Slonimski, P. P. (1989) *Nature*, **337**, 121–122.
49 Gibson, T. J. and Thompson, J. D. (1994) *Nucleic Acids Res.*, **22**, 2552–2556.
50 Fraser, C. M., Gocayne, J. D., Whaite, O., Adams, M. D., Clayton, R. A., Fleischmann, R. D., Bult, C. J., Kerlavage, A. R., Sutton, G., Kelley, J. M. *et al.* (1995) *Science*, **270**, 397–403.
51 St. Johnston, D. (1995) *Cell*, **81**, 161–170.
52 Kaneko, T., Tanaka, A., Sato, S., Kotani, H., Sazuka, T., Miyajima, N., Sugiura, M. and Tabata, S. (1995) *DNA Res.*, **2**, 153–166.
53 Rauhut, R., Jaeger, A., Conrad, C. and Klug, G. (1996) *Nucleic Acids Res.*, **24**, 1246–1251.
54 Oguro, A., Kakeshita, H., Takamatsu, H., Nakamura, K. and Yamane, K. (unpublished). D64116.
55 Waghela, S. D., Rurangirwa, F. R., Mahan, S. M., Yunker, C. E., Crawford, T. B., Barbet, A. F., Burridge, M. J. and McGuire, T. C. (1991) *J. Clin. Microbiol.*, **29**, 2571–2577.
56 Zuber, M., Hoover, T. A., Powell, B. S. and Court, D. L. (1994) *Mol. Microbiol.*, **14**, 291–300.
57 Fleischmann, R. D., Adams, M. D., White, O., Clayton, R. A., Kirkness, E. F., Kerlavage, A. R., Bult, C. J., Tomb, J.-F., Dougherty, B. A., Merrick, J. M. *et al.* (1995) *Science*, **269**, 496–512.
58 Lye, G. and Churcher, C. M. (unpublished). Z66569.
59 Favello, A. D. (unpublished). L14331.